https://doi.org/10.5194/egusphere-2025-2381
Preprint. Discussion started: 11 June 2025

Analysis of the Mother's Day Storm Effects on Equatorial Power Grids Near the Equatorial Electrojet Region

Éfren Mota[1], Edwin Camacho[1], and Luiz Benyosef[1]
[1]COGEO, National Observatory - ON. R. Gen. J. Cristino, 77, Rio de Janeiro, 20921-400, Rj, Brazil
Correspondence: Éfren Mota (efrenmota@on.br)

Abstract. Power transmission lines are susceptible to geomagnetic risks known as geomagnetically induced currents (GICs). These currents arise from rapid variations in the geomagnetic field at Earth's surface, which induce geoelectric fields in the ground and drive GICs into the grounded neutral points of conductive infrastructure such as power transmission networks. In this study, we analyzed the behavior of two equatorial transmission lines —where the Equatorial Electrojet (EEJ) exerts a strong influence on electromagnetic variations —using measured current and voltage records from these lines, along with magnetic data from the geomagnetic superstorm of 10–11 May 2024, one of the most intense events of the past two decades. Magnetic observatories at Tatuoca (TTB), Kourou (KOU), and São Luís (SLZ) were selected to characterize regional field variations via the time derivative of the horizontal geomagnetic component ($d\mathbf{H}/dt$). We then computed Pearson correlation coefficients between two distinct storm phases and the electrical parameters of the lines. The $d\mathbf{H}/dt$ proxy for GIC activity exceeded $\pm$36nT/min at all sites and peaked above 65 nT/min at TTB and SLZ. Strong to very strong correlations emerged during the storm's initial and main phases (first period analized), while correlations weakened to moderate levels during recovery. These findings provide a solid foundation for future studies and inform the development of preventive measures by power-grid operators under intense geomagnetic activity.

1 Introduction

Power transmission networks are critical infrastructure systems, essential for the well-being of modern society and the continuous functioning of everyday technological services. In today's interconnected world, increasing reliance on such systems has become a key vulnerability. The electrical power grid exemplifies a complex socio-technical system —one shaped by tightly coupled natural and human processes —that underpins core societal functions. The widespread integration of digital technologies, including computer and communication networks, as well as cloud infrastructure, has made these interactions more dynamic, with system behavior increasingly influenced by both environmental variability and anthropogenic factors (Che-Castaldo et al., 2021).

Disturbances originating in interplanetary space —such as Coronal Mass Ejections (CMEs) and High-Speed Solar Wind Streams (HSS) —have been shown to affect the stability and resilience of power grids. Notable examples include the 1989 collapse of the Hydro-Québec power system in Canada (Boteler 2019; Bolduc 2002) and the Halloween storm in Africa in October 2003 (Thomson et al., 2010). These events illustrate that grid vulnerabilities are not solely technical in nature but are

https://doi.org/10.5194/egusphere-2025-2381
Preprint. Discussion started: 11 June 2025

also tied to external geophysical drivers, particularly space weather. During geomagnetic storms, interactions between CMEs and Earth's magnetosphere disturb the upper atmosphere, which hosts various large-scale electric current systems. These disturbances cause variations in Earth's surface geomagnetic field, and through Faraday's law of induction Eq. (1), generate geoelectric fields in the ground. These fields can drive unwanted electric currents through grounded infrastructure, including high-voltage power grids (Boteler, 1994, 2001; Kasran et al., 2018a; Pirjola, 2000). These currents, known as Geomagnetically Induced Currents (GICs), can adversely affect power systems by causing transformer overheating, increased reactive power demands, and harmonic generation, potentially leading to system failure (Che-Castaldo et al. 2021; Gaunt and Coetzee 2007).

Large GIC events are typically linked to strong auroral electrojet activity in high-latitude regions (Watari, 2015). However, over the past two decades, several studies have identified GICs effects in low- and mid-latitude regions, particularly in South America (e.g., Barbosa et al. 2014; Caraballo et al. 2013; Espinosa et al. 2023; Trivedi et al. 2007). Nevertheless, the role of the Equatorial Electrojet (EEJ) in such contexts remains underexplored. This study aims to address this gap by investigating the influence of the EEJ on GIC occurrences in regions near the magnetic equator, building on prior research including Carter et al. (2015) and Silva et al. (2024).

$$\nabla \times \mathbf{E} = -\frac{\partial \mathbf{B}}{\partial t} \tag{1}$$

The horizontal configuration of the geomagnetic field, combined with the anisotropic conductivity of the stratified ionosphere, gives rise to distinctive phenomena in the equatorial region. One of the most prominent is the EEJ —a strong eastward electric current that flows within the ionospheric E layer along the magnetic equator during daylight hours at altitudes of 90 to 130 km (Yamazaki and Maute 2017; Zhou et al. 2018). In studies of magnetic variations at low and equatorial latitudes, the EEJ has attracted considerable research interest due to its role in amplifying magnetic signatures in these regions (Silva et al., 2024). Carter et al. (2015) investigated the impact of interplanetary shocks at equatorial latitudes and demonstrated that their geomagnetic signatures are significantly enhanced by EEJ activity. Additionally, Fiori et al. (2014) noted that, although high rates of geomagnetic field variation (dB/dt) are more typically associated with substorm events in high-latitude regions, GICs can also occur at low and mid-latitudes —albeit less frequently and generally with lower intensities.

Given the vulnerability of power transmission lines to the effects of GICs in regions near the magnetic equator, research focused on evaluating space weather conditions during geomagnetic storms can provide valuable input to power system operators developing strategies for scenarios of intense geomagnetic activity. In this context, the use of raw electrical data —derived from the time series of current and voltage measurements from transmission lines —is proposed for the first time as a potentially useful approach for understanding the issue, with possible contributions to both the scientific literature and the power sector.

This study aims to investigate potential correlations between electrical parameters (current and voltage from two power transmission lines) and magnetic parameters (the H component of the geomagnetic field) in the EEJ region during the geomagnetic superstorm of May 10 –11, 2024 —known as the "Mother's Day Storm." This event was analyzed using the respective time series of the involved datasets. To evaluate the magnetic conditions of the regions near the transmission lines, the time derivative of the H component of the geomagnetic field ($d\mathbf{H}/dt$) was calculated for each magnetic observatory (TTB, KOU, and

https://doi.org/10.5194/egusphere-2025-2381
Preprint. Discussion started: 11 June 2025

SLZ). This work is motivated by the need to evaluate the extent to which geomagnetic disturbances correlate with fluctuations in electrical parameters on transmission lines located in low-latitude areas near the EEJ region.

The structure of this work is organized as follows: Section 2 introduces the dataset employed in this study, detailing the characteristics and geographic location of the analyzed power transmission lines, as well as the magnetic observatories selected for investigation. Section 3 describes the methodology used to compute the time derivative of the H component at each magnetic observatory, along with the procedure for calculating the Pearson correlation coefficients between the variables under analysis. Section 4 presents the results, including the calculated $d\mathbf{H}/dt$ values at each observatory and the corresponding correlation coefficients. Section 5 contains the discussion, subdivided into two subsections, each addressing specific aspects of the results. Finally, Section 6 provides the concluding remarks of this study.

2 Datasets

The geomagnetic storm of 10 –11 May 2024, regarded as the most intense event of Solar Cycle 25 so far, reached a minimum Dst index of -412 nT and a Kp index of 9 (see Figure 1). The storm was initiated by the impact of a coronal mass ejection (CME) on Earth's magnetosphere at 17:05 UTC on 10 May, marked by a storm sudden commencement (SSC). This CME originated from the solar active region $AR3664$ and reached the L1 Lagrange point at 16:34 UTC. Its arrival was recorded globally by ground-based magnetometer networks. A second CME reached L1 at 21:36 UTC and impacted Earth at 22:21 UTC on the same day (Tulasi Ram et al., 2024).

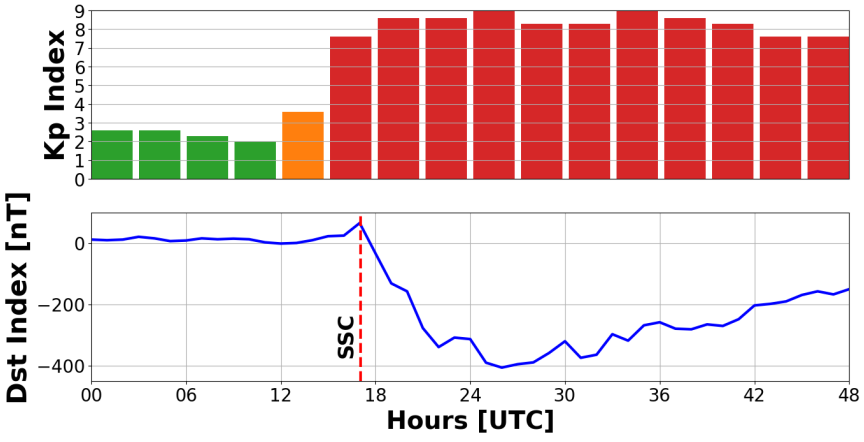

Figure 1. Multi-panel visualization of geomagnetic activity during the 10–11 May 2024 storm, featuring: (upper) Kp index progression, (bellow) Dst index variation.

https://doi.org/10.5194/egusphere-2025-2381
Preprint. Discussion started: 11 June 2025

This study incorporates both electrical and magnetic data. For the magnetic analysis, the horizontal component (H) of the geomagnetic field was selected, as it typically presents the highest amplitude and is particularly sensitive to magnetosphere–ionosphere coupling effects. The magnetic data used were obtained from selected ground-based observatories and sampled at a 1-minute cadence.

2.1 Ground-Based

2.1.1 Power transmission lines

The electrical data analyzed in this study consist of current and voltage measurements from two power transmission lines: Altamira/Transamazônica C1 (TMAT-01) and Altamira/Transamazônica C2 (TMAT-02), both located in the state of Pará, northern Brazil (see table 1 and figure 2). These datasets were provided by the regional energy utility ELETRONORTE and were sampled at 5-minute intervals. The TMAT–01 and TMAT-02 transmission lines run in parallel and therefore share similar geomagnetic coordinates. Each line spans approximately 181.8 km, with identical endpoints at the same substations. They operate at the same voltage level (230 kV) and are equipped with comparable electrical components. Among these components are current transformers (CTs) and potential transformers (PTs), which are responsible for acquiring the operational measurements used in this study. Table 1 lists the magnetic coordinates, latitude Dip [1], sampling rate, and voltage for each power transmission line.

Power transmission line	Code	Country/State	Magnetic lat. (°N)	Magnetic lon. (°E)	Latitude dip (°N)	Sampling rate	Voltage
Altamira/Transamazonic C1	TMAT-01	Brazil/Pará	-1.57	19.49	-1.94	5 min	230 kV
Altamira/Transamazonic C2	TMAT-02	Brazil/Pará	-1.57	19.49	-1.94	5 min	230 kV

Table 1. Detailed information about the power transmission lines.

2.1.2 Magnetic observatories

Figure 2 illustrates the geographic locations of the magnetic observatories utilized in this study: Tatuoca (TTB) and Kourou (KOU), both integral components of the INTERMAGNET (International Real–time Magnetic Observatory Network)[2] initiative. Additionally, data were sourced from the São Luís (SLZ) magnetic station, which is part of the EMBRACE Magnetometer Network (Embrace MagNet)[3], developed by the Brazilian Study and Monitoring of Space Weather Program to enhance magnetic field monitoring across South America. Notably, SLZ is geographically the second closest observatory to the power transmission lines analyzed in this research. For the purposes of this study, the term "observatory" will be employed to refer collectively to both fully equipped observatories and magnetometer stations, acknowledging the technical distinctions between these facilities.

[1] https://geomag.bgs.ac.uk/data_service/models_compass/coord_calc.html
[2] www.intermagnet.org/index-eng.php
[3] https://www2.inpe.br/climaespacial/portal/en/

https://doi.org/10.5194/egusphere-2025-2381
Preprint. Discussion started: 11 June 2025

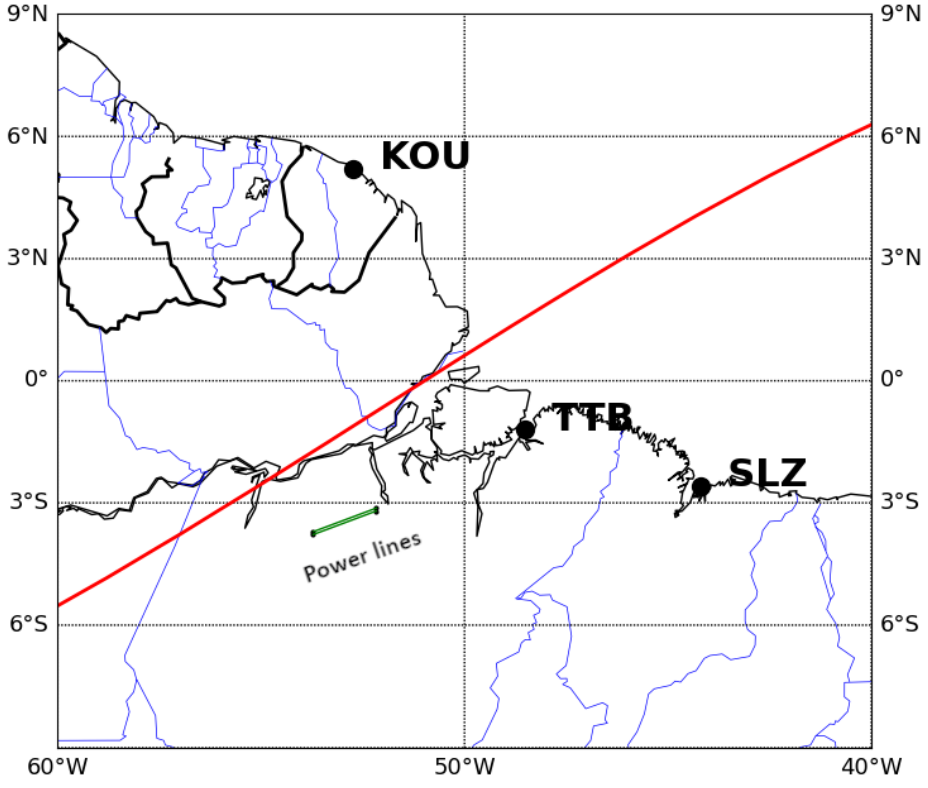

Figure 2. Region of the selected transmission lines (green) and the magnetic observatories (black) used in the research, highlighting the EEJ (red line) crossing the area during the year 2024.

Detailed information about each magnetic observatory used in this work is presented in table 2, with magnetic coordinates provided in the geomagnetic reference system using the 13th generation IGRF model for 2024 to offer more detailed spatial context. The selection of these specific observatories considered their proximity to the transmission lines to preserve similarity in magnetic field morphology and variations near the power lines. Additionally, for evaluating H component variations, observatories located within $\pm 3°$ of the magnetic equator and at low latitudes (6°–9° from the magnetic equator) are considered ideal when accounting for EEJ influence (Soares et al., 2018). Although KOU and SLZ are farther from the transmission lines compared to TTB, were included to allow a comparative analysis of the dynamics of geomagnetic variations between observatories near the EEJ during the period analyzed.

Although the magnetic observatories used in this study are not located in the immediate vicinity of the transmission lines, previous research (Barbosa et al., 2014; Trivedi et al., 2007) has shown that reasonable distance ranges can be considered valid, provided that similarities in the geomagnetic field are preserved in the regions analyzed. For instance, Barbosa et al. (2014) used a separation of approximately 740 km between the Vassouras (VSS) magnetic observatory and the transmission

https://doi.org/10.5194/egusphere-2025-2381
Preprint. Discussion started: 11 June 2025

line addressed in their study (Itumbiara–São Simão), justifying this choice based on the coherence of regional geomagnetic field behavior during storm events.

Magnetic observatory	Country	Magnetic lat. (°N)	Magnetic lon. (°E)	Latitude dip (°N)	Sampling rate	Distance to lines
Tatuoca (TTB)	Brazil	-2.13	23.90	-2.62	1 min	∼460 km
Kourou (KOU)	French Guiana	6.02	22.03	5.87	1 min	∼925 km
São Luís (SLZ)	Brazil	-5.70	23.33	-6.57	1 min	∼977 km

Table 2. Detailed information about the magnetic observatories.

3 Methodology

3.0.1 Time derivative

To assess the amplitude of geomagnetic variations in the vicinity of the transmission lines, this study calculated the time derivative of the horizontal geomagnetic field component ($d\mathbf{H}/dt$), as expressed in Eq. (2). This parameter is a widely recognized proxy for evaluating the potential occurrence of GICs (Viljanen et al., 2001). In high latitude regions, $d\mathbf{H}/dt$ values exceeding 30 nT/min are typically considered indicative of possible GIC activity (Anuar et al. 2019; Kasran et al. 2018b). However, such thresholds can also be reached at lower latitudes, depending on the intensity of geomagnetic disturbances. For instance, Barbosa et al. (2014) recorded *Hx* component amplitudes surpassing 40 nT/min at the mid latitude Vassouras magnetic observatory during the 7–10th November 2004 magnetic storm (Dst $\sim$ -370 nT). Since intense GICs are generally correlated with high $d\mathbf{H}/dt$ values, quantifying this parameter in low-latitude regions is especially relevant. Although large $d\mathbf{H}/dt$ values are more frequently observed at high latitudes—primarily associated with auroral and substorm —related ionospheric currents —their occurrence near the magnetic (Dip) equator warrants closer examination. This is due to the potential modulation of these variations by the EEJ, a phenomenon unique to equatorial latitudes.

$$d\mathbf{H}/dt = f'(t) = \lim_{\Delta t \to 0} \frac{f(t+\Delta t) - f(t)}{\Delta t} \tag{2}$$

where $\Delta t = 1$ minute sampling rate.

During periods of intense geomagnetic activity, abrupt disturbances in ionospheric current systems —often triggered by CME impacts on Earth's magnetosphere —can be monitored through ground-based measurements of the H component variation at magnetic observatories (Russell 2001). Recent studies (Carter et al. 2015; Oliveira et al. 2018; Silva et al. 2024) underscore the significant role of the EEJ in modulating magnetic field variations at low and equatorial latitudes. These findings raise important questions regarding the susceptibility of power transmission lines to GIC generation in regions close to the magnetic equator (Oliveira et al. 2018).

https://doi.org/10.5194/egusphere-2025-2381
Preprint. Discussion started: 11 June 2025

3.0.2 Pearson's correlation coefficient

Given that the transmission lines analyzed in this study are located close to the magnetic equator (see Table 1) and acknowledging the potential influence of the EEJ in promoting GICs near this region, it is reasonable to explore possible correlations between electrical and geomagnetic variables during geomagnetic storm conditions. To objectively quantify such relationships, Pearson's correlation coefficient (Eq. 3) was used as a statistical tool to verify correspondences in terms of distances between the variables analyzed. This measure assesses the linear relationship between two time series and returns a value (denoted as Pearson correlation coefficient, r) within the interval [-1, 1], where a perfect correlation of –1 or +1 means that all the data points lie exactly on a straight line. Conversely, r = 0 implies no linear association between the variables (Duarte et al. 2019; Schober et al. 2018). In this analysis, the time series of the H component was treated as the independent variable x, and the corresponding time series of electrical parameters —either current or voltage —as the dependent variable y, in accordance with the formulation presented in Eq. (3):

$$r_{x,y} = \frac{\sum_{i=1}^{N}(x_i - \overline{x})(y_i - \overline{y})}{\sqrt{\sum_{i=1}^{N}(x_i - \overline{x})^2 (y_i - \overline{y})^2}} \tag{3}$$

The correlation analyses were conducted over two distinct intervals of the geomagnetic storm:

1. Initial and main phases: This period corresponds to the first interval highlighted in figures 3 and 4 (indicated in yellow). Pearson correlation coefficients were calculated separately between the magnetic data and each electrical parameter (current and voltage), covering the interval from the storm sudden commencement (10 May at 17:05 UTC) to the moment when the H component of the geomagnetic field reached its minimum (10 May at 22:55 UTC).

2. Recovery phase: this corresponds to the second period analyzed in the figures 3 and 4 (indicated in light orange). The same analytical procedure was applied during the storm's recovery phase, from 23:00 UTC on 10 May to 23:55 UTC on 11 May.

It is important to note that for each of the analyzed periods, two separate correlation analyses were performed for each transmission line: one correlating current with the H component, and another correlating voltage with the H component. For the electrical data time series (see Figure 4), the analyzed periods correspond to those of the geomagnetic storm time series shown in Figure 2, with identical highlighted intervals.

https://doi.org/10.5194/egusphere-2025-2381
Preprint. Discussion started: 11 June 2025

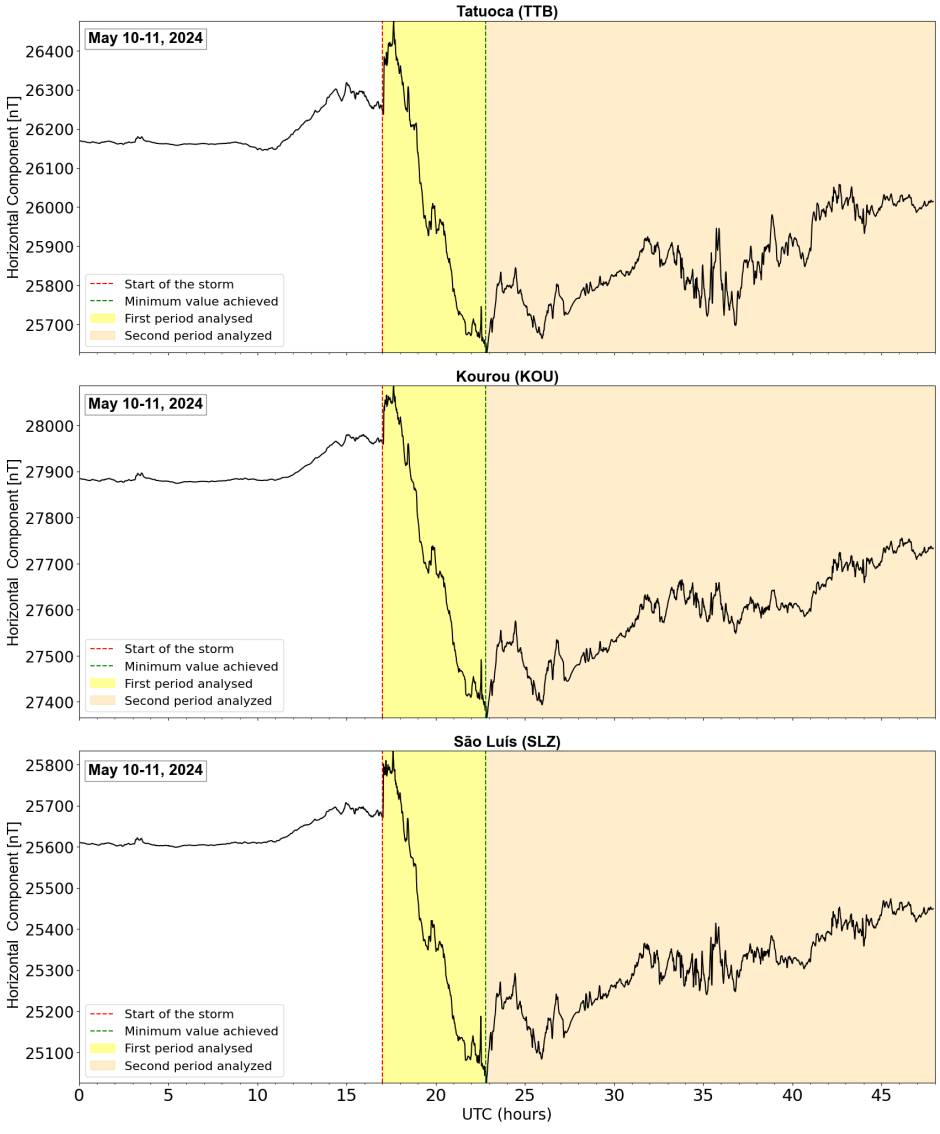

Figure 3. Time series of the geomagnetic storm from 10–11 May 2024 for the magnetic observatories used in this study. The highlighted areas correspond to the first and second analysis periods in the correlation stage between magnetic and electrical data.

https://doi.org/10.5194/egusphere-2025-2381
Preprint. Discussion started: 11 June 2025

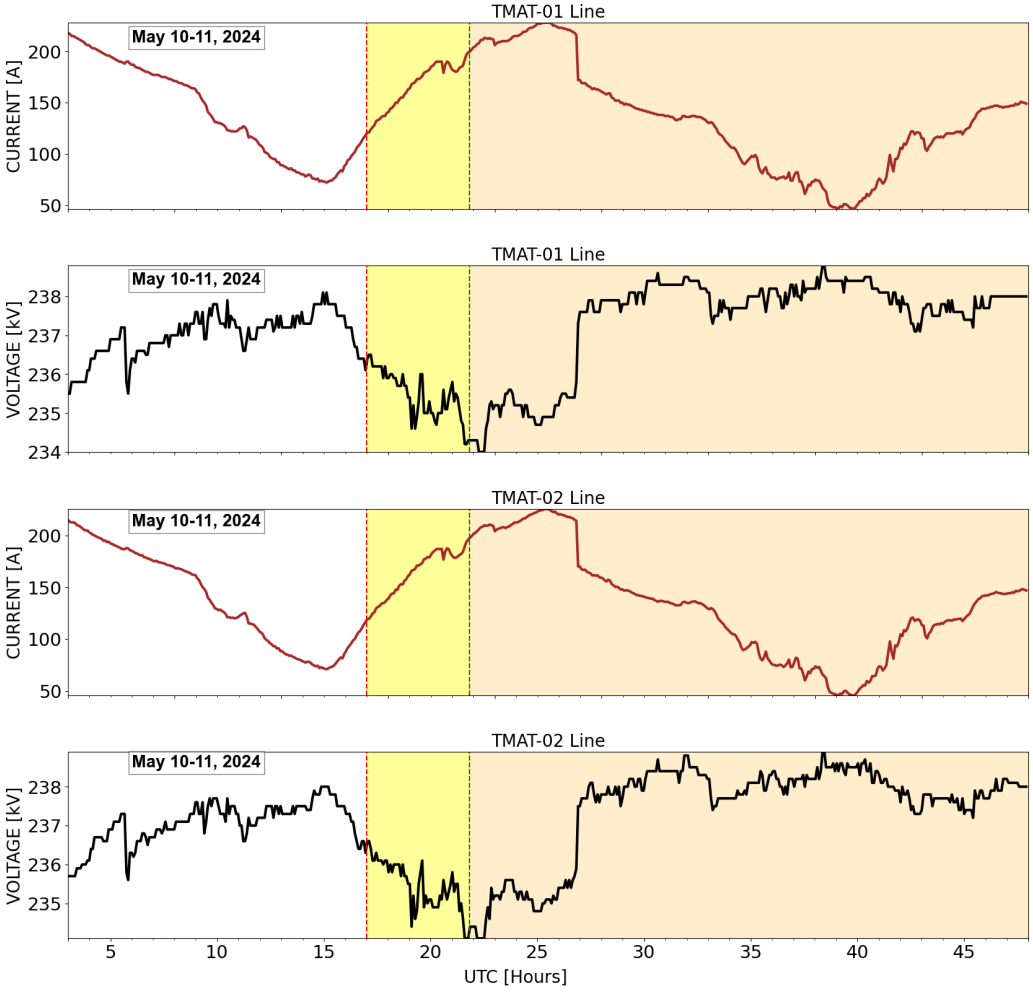

Figure 4. Time series of current and voltage values for the TMAT-01 and TMAT-02 power transmission lines. The highlighted areas correspond to the same period marked in Figure 3.

4 Results

4.1 Time derivative of the Horizontal Geomagnetic Field ($d\mathbf{H}/dt$)

To identify potential occurrences of GICs, we adopted a threshold of 30 nT/min for the time derivative of the horizontal geomagnetic field component ($d\mathbf{H}/dt$), as suggested by Anuar et al. (2019) and Kasran et al. (2018b). All observatories recorded a characteristic $d\mathbf{H}/dt$ peak coinciding with the storm sudden commencement (SSC) at 17:05 UTC on May 10, triggered by the arrival of the first coronal mass ejection (CME) at Earth. Specifically, the Tatuoca (TTB) and São Luís (SLZ) observatories recorded amplitudes exceeding 65 nT/min, while Kourou (KOU) exhibited a maximum amplitude below 40 nT/min. Despite differences in amplitude, all magnetic stations showed similar temporal patterns (see Figure 5).

https://doi.org/10.5194/egusphere-2025-2381
Preprint. Discussion started: 11 June 2025

Given these observations, and considering the established use of $d\mathbf{H}/dt$ as a proxy for GIC inductions, it is reasonable to infer the presence of GICs during the analyzed period. This inference is further supported by studies indicating that $d\mathbf{H}/dt$ values exceeding 30 nT/min are associated with increased GIC activity, even at low latitudes (Anuar et al., 2019; Kasran et al., 2018b).

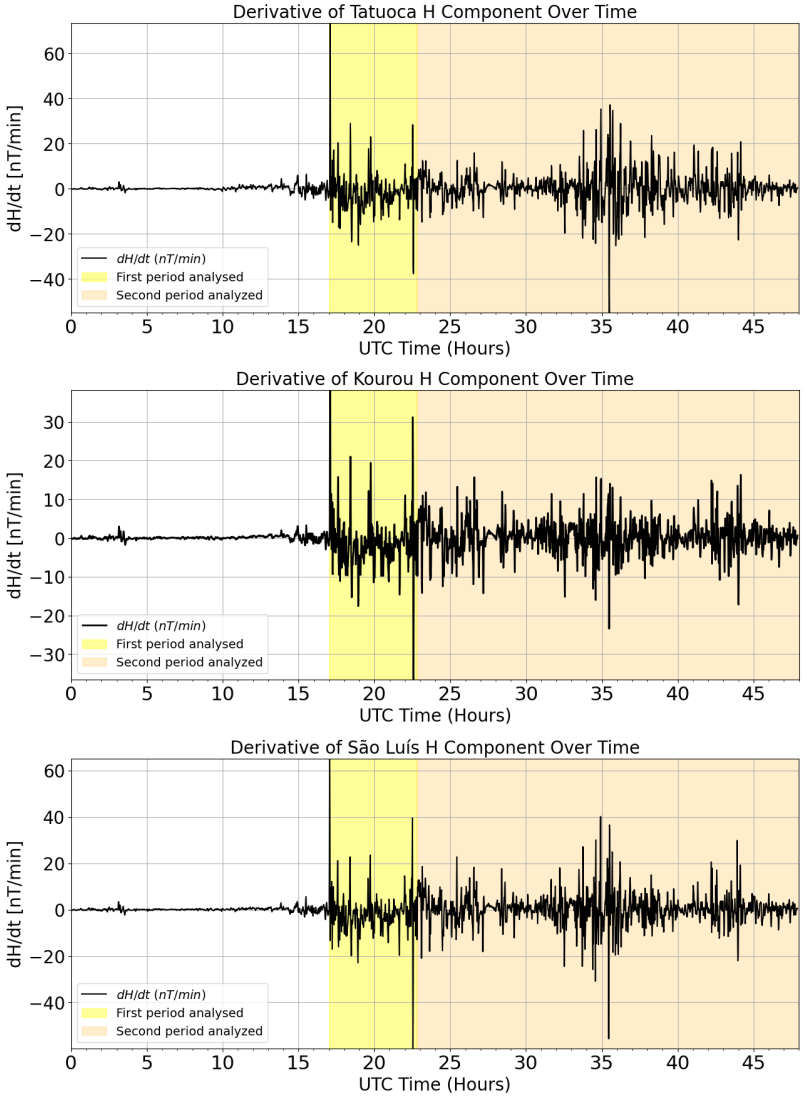

Figure 5. Derivative of the H component for each observatory station. The highlighted areas correspond to the same periods analyzed in Figures 3 and 4.

https://doi.org/10.5194/egusphere-2025-2381
Preprint. Discussion started: 11 June 2025

4.2 Pearson's correlation coefficient

As previously mentioned, the electrical data were sampled at 5-minute intervals. Therefore, the geomagnetic storm time series was resampled to the same 5-minute resolution to ensure consistency during this phase of the analysis.

4.2.1 First period analyzed

Pearson's correlation coefficient was calculated for two distinct time intervals. The first corresponds to the onset of the geomagnetic storm at 17:05 UTC and includes the entire initial and main phases, extending slightly into the beginning of the recovery phase. This interval ends at 22:55 UTC on May 10, when the H component of the geomagnetic field reaches its minimum value. The correlation results for this first period are presented in figures 6, 7 and 8, corresponding to the TTB, KOU, and SLZ observatories, respectively.

All Pearson correlation coefficients (r) were interpreted according to the strength classification proposed by Schober et al. (2018). Among the strongest correlations, the r values between the H component and Current range from -0.95 (Figures 7A/C and 8A/C) to -0.94 (Figures 6A and 6C), indicating a very strong negative correlation. Notably, the H component and Current correlations for both SLZ and KOU magnetic stations reached identical peak values of r = -0.95. In contrast, correlations between the H component and voltage, although of opposite sign, also demonstrated strong relationships, with positive r values ranging from 0.82 to 0.84. The strongest of these was observed at the SLZ observatory, with r = 0.84 (Figure 8D), indicating a strong positive correlation between voltage and the geomagnetic H component.

https://doi.org/10.5194/egusphere-2025-2381
Preprint. Discussion started: 11 June 2025

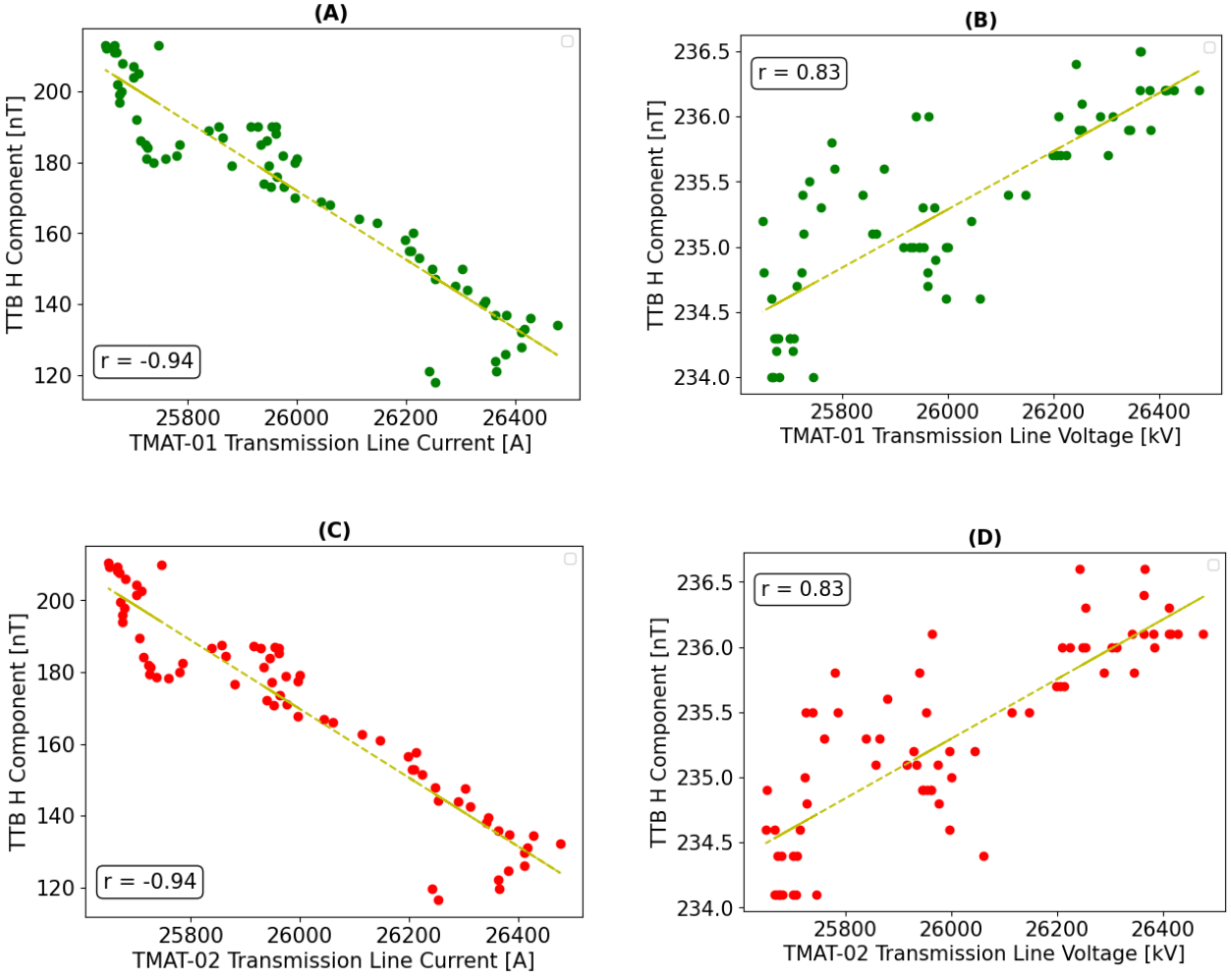

Figure 6. Pearson correlation analysis between variables: H component (TTB) × Current (**A** and **C**); H component (TTB) × Voltage (**B** and **D**) for their respective transmission lines. The yellow dashed line represents a trend line.

https://doi.org/10.5194/egusphere-2025-2381
Preprint. Discussion started: 11 June 2025

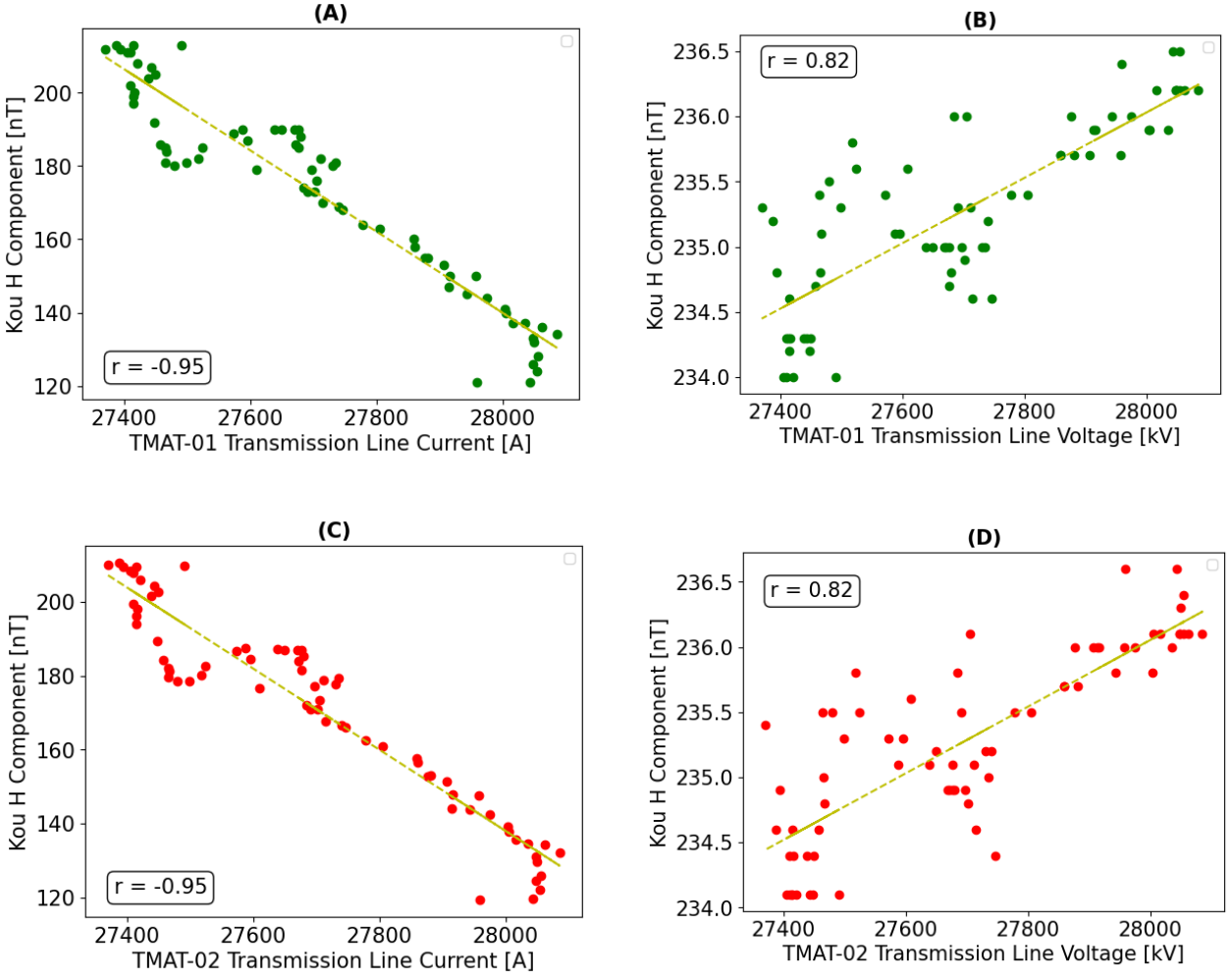

Figure 7. Pearson correlation analysis between variables: H component (KOU) × Current (**A** and **C**); H component (KOU) × Voltage (**B** and **D**) for their respective transmission lines. The yellow dashed line represents a trend line.

https://doi.org/10.5194/egusphere-2025-2381
Preprint. Discussion started: 11 June 2025

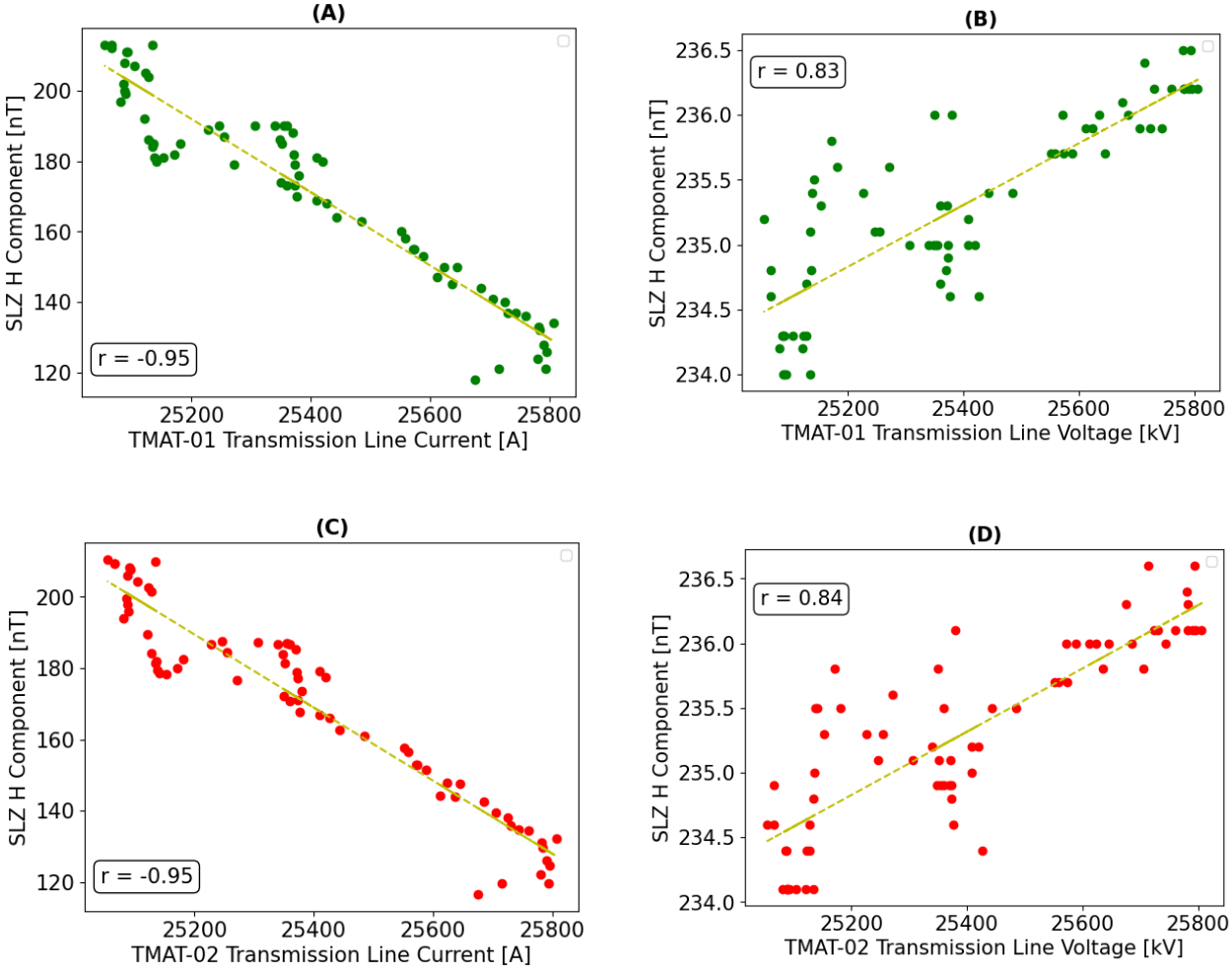

Figure 8. Pearson correlation analysis between variables: H component (SLZ) × Current (**A** and **C**); H component (SLZ) × Voltage (**B** and **D**) for their respective transmission lines. The yellow dashed line represents a trend line

4.2.2 Second period analyzed

The second analysis period corresponds entirely to the recovery phase of the geomagnetic storm, extending from 23:00 UTC on 10 May to 23:55 UTC on 11 May. The correlation results for this interval are presented in figures 9, 10, and 11, corresponding to the Tatuoca (TTB), Kourou (KOU), and São Luís (SLZ) observatories, respectively. In comparison with the first analysis period, the Pearson correlation coefficient (r) values during the recovery phase showed a notable decrease, indicating weaker statistical associations. According to the classification by Schober et al. (2018), the correlations ranged from weak (r = 0.10–0.39) to moderate (r = 0.40–0.69).

https://doi.org/10.5194/egusphere-2025-2381
Preprint. Discussion started: 11 June 2025

The strongest correlation between the H component and current was observed at the SLZ observatory, where both transmission lines exhibited moderate negative correlations of r = –0.55 (Figures 11A and 11C). In contrast, the weakest correlation was recorded between the H component at TTB and the current measured on the TMAT–01 line, with r = –0.39 (Figure 9A), classified as weak. Regarding the relationship between the H component and voltage, the highest positive correlation was also observed at the SLZ observatory for the TMAT–01 line, with r = 0.55 (Figure 11D), indicating a moderate positive association. The lowest voltage correlation was recorded at TTB for the TMAT–02 line, with r = 0.43 (Figure 9D), which still falls within the moderate correlation range.

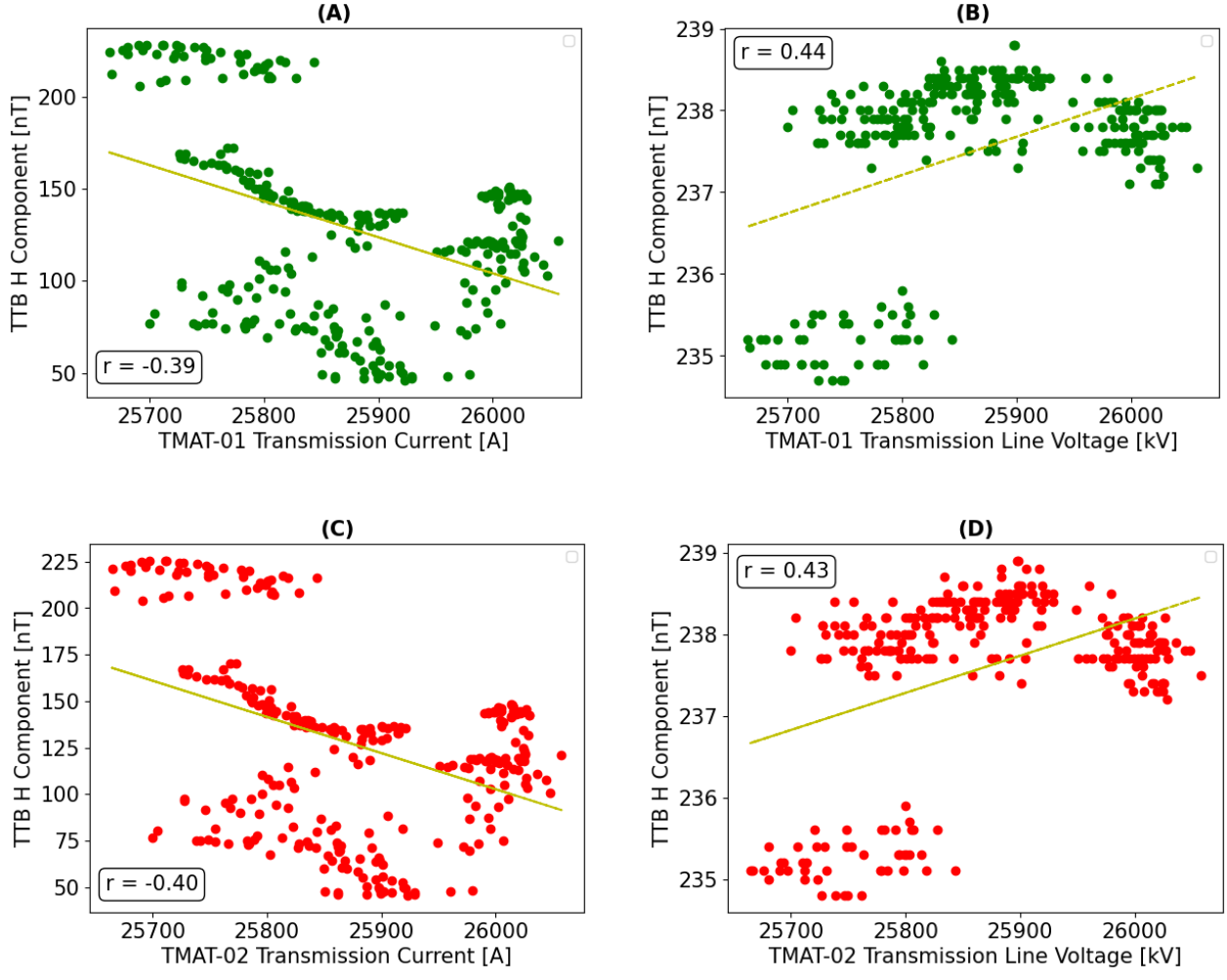

Figure 9. Pearson correlation analysis between variables: H component (TTB) × Current (**A** and **C**); H component (TTB) × Voltage (**B** and **D**) for their respective transmission lines. The yellow dashed line represents a trend line.

https://doi.org/10.5194/egusphere-2025-2381
Preprint. Discussion started: 11 June 2025

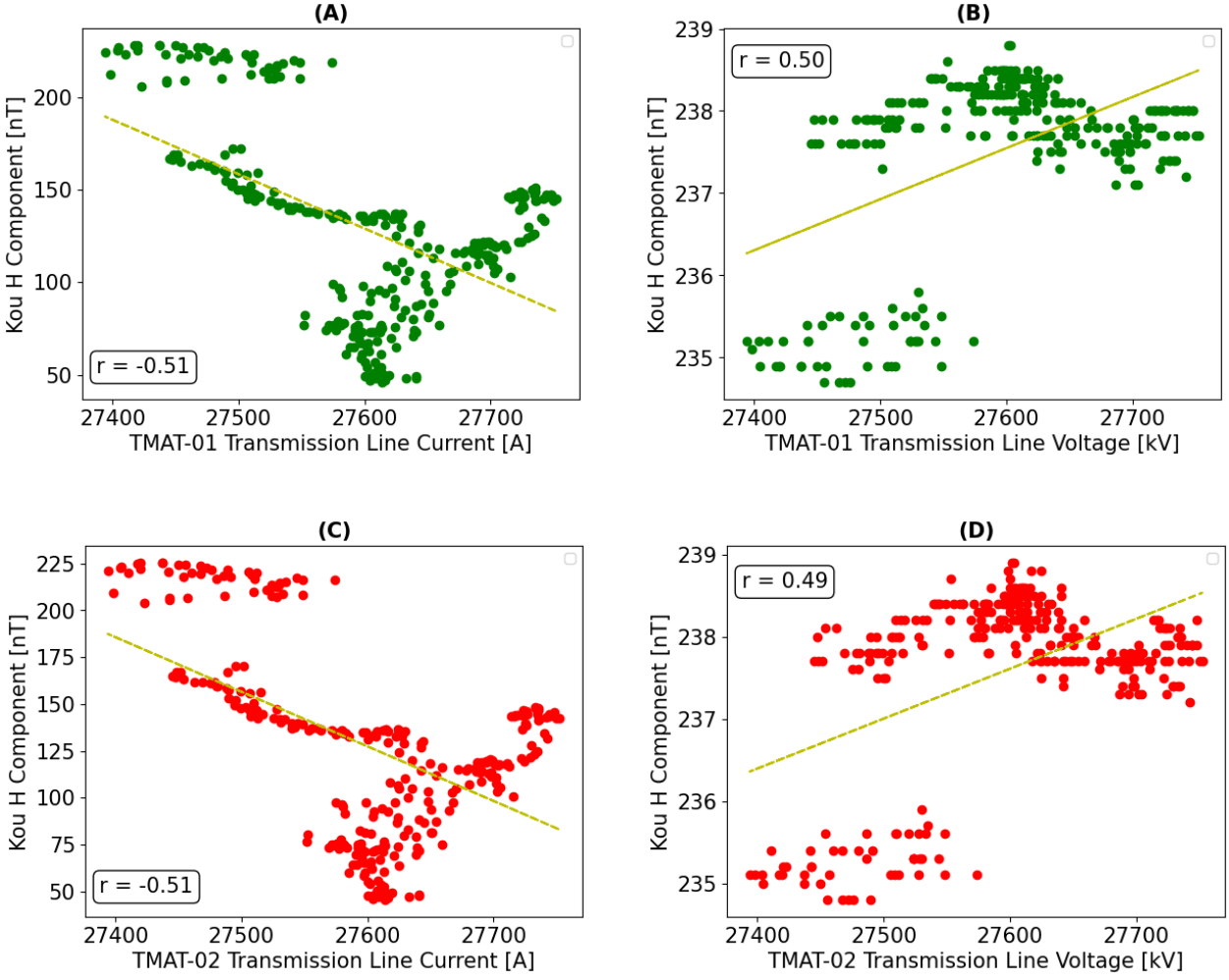

Figure 10. Pearson correlation analysis between variables: H component (KOU) × Current (**A** and **C**); H component (KOU) × Voltage (**B** and **D**) for their respective transmission lines. The yellow dashed line represents a trend line.

The correlation coefficients (r) between the electrical and magnetic parameters recorded at the Kourou (KOU) observatory exhibited highly consistent values across both transmission lines. Specifically, a moderate negative correlation was observed between the electric current and the H component of the geomagnetic field, with r = –0.51. Regarding the relationship between voltage and the H component, positive correlations of similar magnitude were identified: r = 0.50 for the TMAT–01 line and r = 0.49 for the TMAT–02 line (see Figure 10).

https://doi.org/10.5194/egusphere-2025-2381
Preprint. Discussion started: 11 June 2025

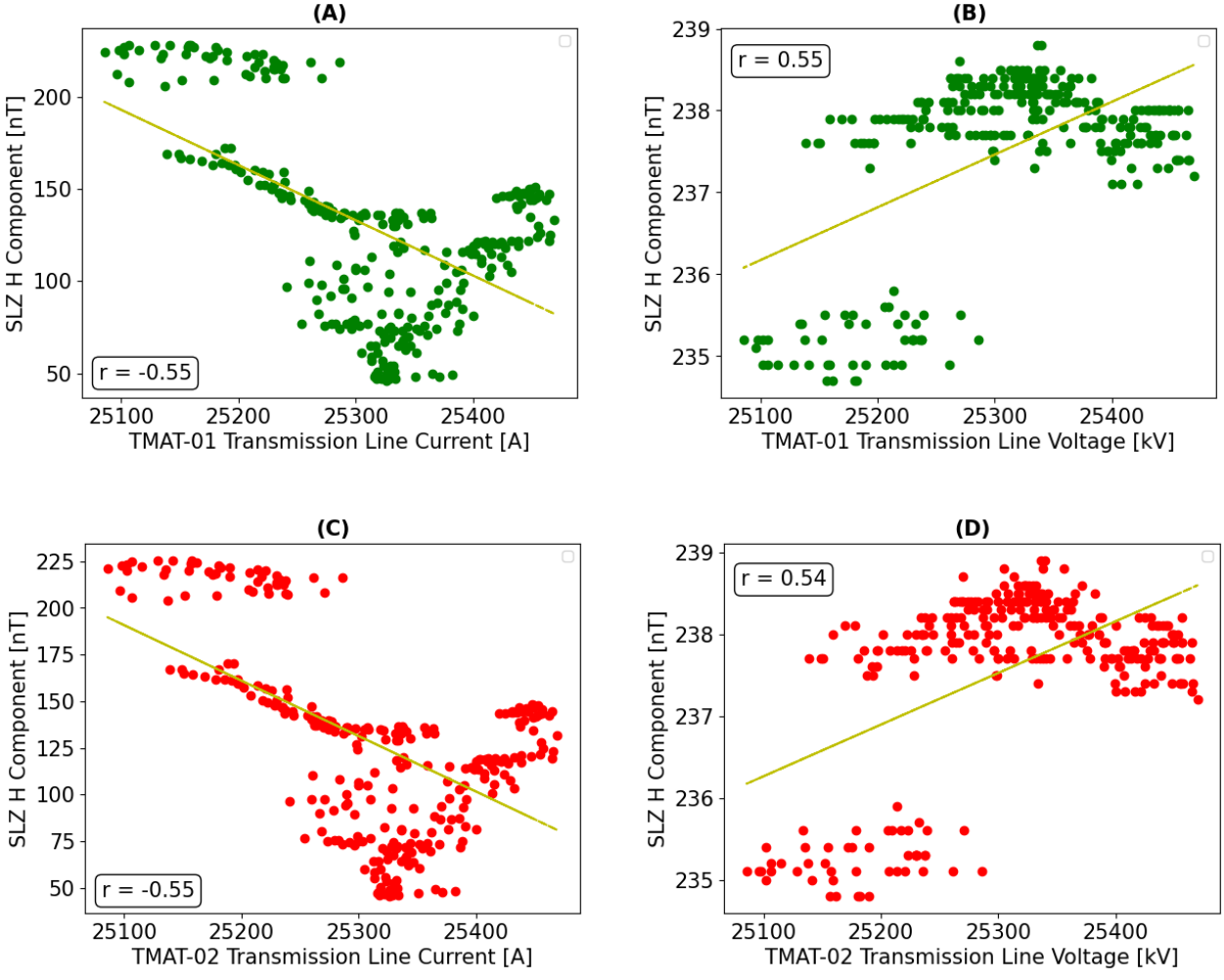

Figure 11. Pearson correlation analysis between variables: H component (SLZ) × Current (**A** and **C**); H component (SLZ) × Voltage (**B** and **D**) for their respective transmission lines. The yellow dashed line represents a trend line.

5 Discussion

This study presents an analysis of the time derivative of the horizontal geomagnetic field component $d\mathbf{H}/dt$ at low and equatorial latitudes, with the objective of evaluating the potential for GIC generation in equatorial regions near the analyzed power transmission lines. Additionally, a correlation analysis between magnetic and electrical parameters was conducted to identify
210 possible relationships between the time series of the H component (from each magnetic observatory) and the current and voltage measurements from the transmission lines. These analyses were performed in the context of the geomagnetic storm of May

https://doi.org/10.5194/egusphere-2025-2381
Preprint. Discussion started: 11 June 2025

10–11, 2024 —commonly referred to as the "Mother's Day Storm" —which stands as the most intense event of Solar Cycle 25 to date, with a maximum Kp index of 9 and a minimum Dst index of –412 nT.

Even though SLZ and KOU are located in low-latitude regions (unlike TTB, which lies at the equatorial latitude and is closer to the transmission lines) this spatial separation does not appear to be a relevant issue, as the geomagnetic storm time series and $d\mathbf{H}/dt$ values recorded at all three observatories (KOU, TTB and SLZ) exhibit consistent and similar behavior. This similarity indicates that the geomagnetic field in the study region can be considered uniform with respect to variations in the horizontal component (H). Therefore, the use of these observatories appears to be a reasonable and appropriate approach for characterizing the geomagnetic environment in this study.

While the investigation of $d\mathbf{H}/dt$ peaks and their potential correspondence with electrical parameters forms the core of this study, a comprehensive interpretation must also consider additional factors. A crucial aspect relates to the magnetic location of the observatories, since the intensity of geomagnetic variations is strongly influenced by their proximity to the magnetic equator. Stations located within or near the EEJ region are particularly sensitive to ionospheric current dynamics, which can amplify magnetic field disturbances. Moreover, the specific characteristics of the geomagnetic storm under analysis are also significant. The event analyzed here was preceded by a SSC, a phenomenon known to play a critical role in GICs induction at low and equatorial latitudes. This has been demonstrated in prior studies (Carter et al. 2015; Kappenman 2003; Zhang et al. 2015) which support the methodological approach adopted in this research and highlight the relevance of examining SSC-related effects when assessing GICs vulnerability in low- and equatorial-latitudes power systems.

5.1 Implications of the peak $d\mathbf{H}/dt$ values

The $d\mathbf{H}/dt$ peaks observed at all magnetic observatories analyzed in this study exceeded the threshold of 30 nT/min proposed by Anuar et al. (2019) and Kasran et al. (2018b), as shown in figure 5. Our analysis is based on the assumption that the EEJ can amplify magnetic variations during geomagnetic storms in regions near the magnetic equator, thereby increasing the vulnerability of power infrastructure in these areas to GICs (Carter et al., 2015). At all observatories, the highest $d\mathbf{H}/dt$ peaks occurred immediately following the interplanetary shock associated with the SSC at 17:05 UTC on 10 May, consistent with the findings of Carter et al. (2015) and Fiori et al. (2014). Notably, the initial and main phases of the storm (from 17:05 to approximately 22:00 UTC) occurred predominantly during daytime local time (LT = UTC –3) at the geographic locations of the transmission lines and the SLZ, KOU, and TTB observatories—conditions that favor enhanced ionospheric conductivity and EEJ activity.

Rout et al. (2025) reported clear evidence of equatorial ionization anomalies during the May 10–11, 2024 geomagnetic storm, including a pronounced intensification of the EEJ recorded at the Jicamarca Observatory (11.95° S, 76.97° W; MLAT = 0.6° N) in the South American sector. A significant enhancement of the magnetic field associated with the EEJ was observed, peaking at approximately ~ 275 nT at 17:40 UTC —around 35 minutes after the SSC. This indicates that during the event the EEJ responded dynamically to ionospheric/magnetospheric disturbances in a manner that could have contributed to GICs induction in regions near the magnetic equator.

https://doi.org/10.5194/egusphere-2025-2381
Preprint. Discussion started: 11 June 2025

The $d\mathbf{H}/dt$ values reported in this study further reinforce the potential risk of GIC occurrence in low- and equatotial-latitude regions (such as those where the studied transmission lines are located) as they are comparable to values documented in earlier studies. Barbosa et al. (2014) found $d\mathbf{H}/dt$ peaks exceeding 100 nT/min during the 29th October until 1st November 2003 magnetic storm ("Halloween magnetic storm"), with the highest magnetic field variations coinciding with modeled peak GICs amplitudes on a low-latitude transmission line. As expected, due to the influence of the EEJ, the highest $d\mathbf{H}/dt$ values in our study were recorded at the Tatuoca (TTB) observatory, the station nearest to the magnetic equator. This finding aligns with the observations of Abd Latiff and Jusoh (2021), who noted that average $d\mathbf{H}/dt$ values tend to increase as magnetic latitude approaches the dip equator.

Interestingly, the $d\mathbf{H}/dt$ peak recorded at São Luís (SLZ) reached approximately 66 nT/min, a magnitude comparable to the 73 nT/min recorded at TTB. Given SLZ's position farther south of the magnetic equator, lower $d\mathbf{H}/dt$ values would typically be expected. However, this apparent anomaly may be explained by the findings of Rigoti et al. (1999), who analyzed EEJ morphology using data from an array of 29 magnetometers deployed across northern and northeastern Brazil. Their study revealed that the EEJ center is, on average, displaced approximately 21 km southward from the magnetic equator, with occasional displacements of up to 62 km. Such a southward shift could account for the elevated $d\mathbf{H}/dt$ values recorded at SLZ despite its relatively higher magnetic latitude compared to TTB. In contrast, the Kourou (KOU) observatory, located farther from the EEJ center, recorded maximum $d\mathbf{H}/dt$ values of approximately 38 nT/min (Figure 5, middle panel) —significantly lower than those observed at TTB and SLZ. This supports the interpretation that proximity to the EEJ strongly influences the intensity of geomagnetic variations in equatorial regions.

The geomagnetic conditions observed during the 10–11 May 2024 storm were conducive to GIC occurrence, even in low- and equatorial–latitude regions. Such extreme events (classified as superstorms) can generate significant ionospheric currents, particularly through EEJ dynamics, and thus represent a substantial risk to power systems in these regions (Zhang et al., 2022). Given the global impact of geomagnetic superstorms, proactive measures —including real-time monitoring, infrastructure hardening, and maintenance planning —should be considered essential for the protection of power grid infrastructure, even at latitudes traditionally considered less vulnerable.

5.2 Possible correspondences between Space Weather parameter and Electrical parameters

In many space weather studies, correlation techniques are commonly employed to analyze relationships between parameters associated, for instance, with the solar wind, CMEs, GICs, $d\mathbf{H}/dt$, among others (Silva et al. 2024; Samwel and Miteva 2023; Smith et al. 2022). During intense events such as geomagnetic storms, many of these quantities vary as a function of one another, making correlation analysis a valuable tool for investigating such interdependencies. In the present study, this technique was applied to examine possible associations between variations in the H component of the geomagnetic field and changes in current and voltage along power transmission lines during the May 10–11, 2024 geomagnetic storm.

Additionally, this analysis was used to support the interpretation of $d\mathbf{H}/dt$ results and to reinforce our underlying hypothesis —based on previous studies —that GICs can develop at low- and equatorial–latitudes, with the EEJ playing a key role in this context (Carter et al., 2015). The correlations identified during the first analyzed period indicate strong associations between

https://doi.org/10.5194/egusphere-2025-2381
Preprint. Discussion started: 11 June 2025

current and the H component, as well as between voltage and the H component, as shown in figures 6, 7, and 8. It is worth noting that, in both periods analyzed, the behavior of the H component, current, and voltage varied distinctly. For example, while current values decreased during the first interval, voltage values increased (see Fig. 4). Within this same time window, the storm's initial and main phases occurred, followed shortly by the minimum H value at the onset of the recovery phase. This dynamic could explain the positive correlation between the H component and voltage, and the negative correlation between current and the H component observed during that period.

Given that the observed correlation coefficients (r values) during the first analysis period were statistically significant (with $r > 0.80$), the strong correlations between the H component and voltage/current suggest that much of the voltage or current variation is directly influenced by the H component during the initial and main phases of the storm. Consequently, it is plausible that these strong correlations, along with $d\mathbf{H}/dt$ values exceeding $|60nT/min|$, are associated with the incidence of GICs in power transmission lines. However, this assertion goes beyond the scope of the present study, which is focused on analyzing the results obtained through the methods employed and the available literature. A more robust confirmation of the presence of GICs in these lines would require the inclusion of additional parameters commonly used in the field, such as the ground resistivity structure and the specific configuration of the analyzed power grid (McKay and Whaler 2006; Pirjola 2002; Pulkkinen et al. 2013).

In the second analysis interval, a general decrease in correlation values was observed (Fig. 9, 10, and 11). The weak correlations between the H component and voltage/current suggest that variations in voltage or current were only slightly influenced by the H component during the storm's recovery phase. Furthermore, at 02:00 UTC on May 11, an increase in high-energy proton flux (>500 MeV) was detected (Hayakawa et al., 2025), causing abrupt fluctuations in the H component time series (see Figure 3), which may have also affected the correlation coefficients (r values) during this period. Although the r values decreased during the second analysis period, $d\mathbf{H}/dt$ peaks exceeding 65 nT/min were still recorded at the TTB and SLZ observatories (Fig. 5). These values alone could indicate conditions favorable for GIC induction and potential risks to the power grid. Nonetheless, this observation lies beyond the scope of the current investigation.

As the first study to analyze raw electrical data in the context of intense geomagnetic activity, the results presented here provide relevant support for future investigations and contribute to the contextualization of the observational data discussed in this research. Moreover, the study highlights the feasibility of using time series of current and voltage as a complementary tool in identifying potential GIC-related effects. Such integration may foster advances in the modeling of electromagnetic coupling and in the development of predictive strategies aimed at mitigating risks to transmission networks in low- and equatorial–latitude regions, which remain relatively understudied.

6 Conclusions

Although the impacts of GICs on power systems are well documented in high-latitude regions, their occurrence and potential effects in areas near the magnetic equator remain significantly underexplored. Transmission lines located in these equatorial

https://doi.org/10.5194/egusphere-2025-2381
Preprint. Discussion started: 11 June 2025

regions —long considered less vulnerable —have started to show signs of susceptibility to geomagnetic disturbances, highlighting the urgent need for focused studies in this specific context.

In this study, the $d\mathbf{H}/dt$ method (widely used in the literature to identify potential GIC occurrences) was applied, along with Pearson correlation analysis, to investigate possible relationships between geomagnetic variations and electrical parameters during the geomagnetic storm of May 10–11, 2024, the most intense event of its kind in the past two decades. This work represents the first known analysis of raw electrical time series data from power transmission lines in correlation with the time series of the H component of the geomagnetic field.

The main conclusions drawn from this study are as follows:

- Exceedance of $d\mathbf{H}/dt$ thresholds: All $d\mathbf{H}/dt$ peaks recorded by the magnetic observatories utilized in this study surpassed the commonly cited threshold of 30 nT/min, which is indicative of potential GICs activity .
- Spatial Variations in $d\mathbf{H}/dt$ Peaks: The most pronounced $d\mathbf{H}/dt$ peaks were observed at the Tatuoca (TTB) and São Luís (SLZ) observatories, likely attributable to their proximity to the core of the EEJ. Conversely, the Kourou (KOU) observatory, situated farther from the EEJ, recorded the lowest peak values.
- Correlation Patterns During Storm Phases: During the initial and main phases of the geomagnetic storm, a strong negative correlation was identified between the horizontal component (H) of the geomagnetic field and electric current, while a strong positive correlation was observed between the H component and voltage.
- Correlation Patterns During Recovery Phase: In the recovery phase of the storm, correlations between the H component and current ranged from moderate to weak, with the weakest correlation noted for the TMAT–02 transmission line. Correlations between the H component and voltage during this phase remained moderately positive.

Our findings demonstrate that, at two observatories (TTB and SLZ) situated near the EEJ region, the time derivative of the horizontal geomagnetic field component ($d\mathbf{H}/dt$) reached magnitudes of approximately $|60\ nT/min|$ during geomagnetic storm events. This rate of change is significant, as elevated $d\mathbf{H}/dt$ values are known to enhance the induction of GICs, which can adversely affect power grid infrastructure. Furthermore, the Pearson correlation coefficients calculated between the analyzed variables indicate a potentially significant relationship, particularly during the initial and main phases of the geomagnetic storm. This suggests a strong coupling of magnetic variations with the electrical parameters of transmission lines in equatorial regions.

These observations underscore the importance of expanding research on GICs, especially in low- and equatorial–latitude regions where the EEJ may serve as a significant source of geomagnetic disturbances. While GICs have been extensively studied in high-latitude areas, their impacts in equatorial zones remain less understood. To validate these findings and enhance our understanding of GIC behavior in equatorial regions, further investigations are necessary. Conducting comparative studies between periods of low and high geomagnetic activity would allow for a more robust characterization of transmission line responses to GICs induction. Such analyses could confirm the consistency of the observed results and provide a comprehensive understanding of how space weather disturbances influence electrical systems near the Equatorial Electrojet Region.

https://doi.org/10.5194/egusphere-2025-2381
Preprint. Discussion started: 11 June 2025

Code availability. The software code used in this study was developed in-house and is based on predefined functions in PYTHON.

Data availability. Data are available from the international repositories (ex. Intermagnet) and from INPE Embrace's site. The electrical data sets are available in: https://doi.org/10.5281/zenodo.15420292 (Mota, 2025).

Author contributions. All authors cooperate in the same proportion in the work.

Competing interests. The authors declare no competing interests.

Acknowledgements. We thank CNPq and the Nacional Observatory for awarding a scholarship to the first author, grant 1013/2023-2. We also acknowledge INTERMAGNET and EMBRACE for providing the data utilized in this study, and ELETROBRAS for supplying essential information and data that significantly contributed to the development of this work. EC received from the Coordenação de Aperfeiçoamento de Pessoal de Nível Superior (CAPES), grant 301114/2024-2.

https://doi.org/10.5194/egusphere-2025-2381
Preprint. Discussion started: 11 June 2025

References

Abd Latiff, Z. I. and Jusoh, M. H.: Analysis of geomagnetically induced currents (GIC) at equatorial region over solar cycle 24, Journal of Electrical and Electronic Systems Research (JEESR), 19, 37–42, https://doi.org/10.24191/jeesr.v19i1.005, 2021.

Anuar, N. M., Kasran, F. M., Abbas, M., Jusoh, M., Ab Rahim, S. E., Hadi, N. A., Yoshikawa, A., Radzi, Z. M., et al.: Assessment of the Geomagnetically Induced Current (GIC) at low latitude region based on MAGDAS data, in: Journal of Physics: Conference Series, vol. 1152, p. 012028, IOP Publishing, https://doi.org/10.1088/1742-6596/1152/1/012028, 2019.

Barbosa, C., Hartmann, G., Katia, J., and Pinheiro, K.: Numerical modeling of geomagnetically induced currents in a Brazilian transmission line, Advances in Space Research, 55, https://doi.org/10.1016/j.asr.2014.11.008, 2014.

Bolduc, L.: GIC observations and studies in the Hydro-Québec power system, Journal of Atmospheric and Solar-Terrestrial Physics, 64, 1793–1802, https://doi.org/https://doi.org/10.1016/S1364-6826(02)00128-1, space Weather Effects on Technological Systems, 2002.

Boteler, D.: Geomagnetically induced currents: present knowledge and future research, IEEE Transactions on Power Delivery, 9, 50–58, https://doi.org/10.1109/61.277679, 1994.

Boteler, D. H.: Space Weather Effects on Power Systems, pp. 347–352, American Geophysical Union (AGU), ISBN 9781118668351, https://doi.org/https://doi.org/10.1029/GM125p0347, 2001.

Boteler, D. H.: A 21st Century View of the March 1989 Magnetic Storm, Space Weather, 17, 1427–1441, https://doi.org/https://doi.org/10.1029/2019SW002278, 2019.

Caraballo, R., Sánchez Bettucci, L., and Tancredi, G.: Geomagnetically induced currents in the Uruguayan high-voltage power grid, Geophysical Journal International, 195, 844–853, https://doi.org/10.1093/gji/ggt293, 2013.

Carter, B. A., Yizengaw, E., Pradipta, R., Halford, A. J., Norman, R., and Zhang, K.: Interplanetary shocks and the resulting geomagnetically induced currents at the equator, Geophysical Research Letters, 42, 6554–6559, https://doi.org/https://doi.org/10.1002/2015GL065060, 2015.

Che-Castaldo, J. P., Cousin, R., Daryanto, S., Deng, G., Feng, M.-L. E., Gupta, R. K., Hong, D., McGranaghan, R. M., Owolabi, O. O., Qu, T., et al.: Critical Risk Indicators (CRIs) for the electric power grid: a survey and discussion of interconnected effects, Environment Systems and Decisions, 41, 594–615, https://doi.org/10.1007/s10669-021-09822-2, 2021.

Duarte, F. S., Rios, R. A., Hruschka, E. R., and de Mello, R. F.: Decomposing time series into deterministic and stochastic influences: A survey, Digital Signal Processing, 95, 102 582, https://doi.org/10.1016/j.dsp.2019.102582, 2019.

Espinosa, K. V., Padilha, A. L., Alves, L. R., Schultz, A., and Kelbert, A.: Estimating geomagnetically induced currents in southern Brazil using 3-D Earth resistivity model, Space Weather, 21, e2022SW003 166, https://doi.org/10.1029/2022SW003166, 2023.

Fiori, R. A. D., Boteler, D. H., and Gillies, D. M.: Assessment of GIC risk due to geomagnetic sudden commencements and identification of the current systems responsible, Space Weather, 12, 76–91, https://doi.org/https://doi.org/10.1002/2013SW000967, 2014.

Gaunt, C. and Coetzee, G.: Transformer failures in regions incorrectly considered to have low GIC-risk, in: 2007 IEEE Lausanne power tech, pp. 807–812, IEEE, https://doi.org/10.1109/PCT.2007.4538419, 2007.

Hayakawa, H., Ebihara, Y., Mishev, A., Koldobskiy, S., Kusano, K., Bechet, S., Yashiro, S., Iwai, K., Shinbori, A., Mursula, K., et al.: The Solar and Geomagnetic Storms in 2024 May: A Flash Data Report, The Astrophysical Journal, 979, 49, https://doi.org/10.3847/1538-4357/ad9335, 2025.

Kappenman, J. G.: Storm sudden commencement events and the associated geomagnetically induced current risks to ground-based systems at low-latitude and midlatitude locations, Space Weather, 1, https://doi.org/https://doi.org/10.1029/2003SW000009, 2003.

https://doi.org/10.5194/egusphere-2025-2381
Preprint. Discussion started: 11 June 2025

Kasran, F. A. M., Jusoh, M. H., Rahim, S. A. E. A., and Abdullah, N.: Geomagnetically Induced Currents (GICs) in Equatorial Region, in: 2018 IEEE 8th International Conference on System Engineering and Technology (ICSET), pp. 112–117, IEEE, https://doi.org/10.1109/ICSEngT.2018.8606391, 2018a.

Kasran, F. A. M., Jusoh, M. H., Yoshikawa, A., and Radzi, Z. M.: The Time Derivative of the Horizontal Geomagnetic Field for the Low Latitude MAGDAS Langkawi Station for the Estimation of Geomagnetically Induced Current, pp. 57–71, Springer Singapore, https://doi.org/10.1007/978-981-10-6574-3_6, 2018b.

McKay, A. and Whaler, K.: The electric field in northern England and southern Scotland: Implications for geomagnetically induced currents, Geophysical Journal International, 167, 613–625, https://doi.org/10.1111/j.1365-246X.2006.03128.x, 2006.

Mota, E.: Electrical dataset, https://doi.org/10.5281/zenodo.15420292, 2025.

Oliveira, D. M., Arel, D., Raeder, J., Zesta, E., Ngwira, C. M., Carter, B. A., Yizengaw, E., Halford, A. J., Tsurutani, B. T., and Gjerloev, J. W.: Geomagnetically Induced Currents Caused by Interplanetary Shocks With Different Impact Angles and Speeds, Space Weather, 16, 636–647, https://doi.org/https://doi.org/10.1029/2018SW001880, 2018.

Pirjola, R.: Geomagnetically induced currents during magnetic storms, IEEE Transactions on Plasma Science, 28, 1867–1873, https://doi.org/10.1109/27.902215, 2000.

Pirjola, R.: Review on the calculation of surface electric and magnetic fields and of geomagnetically induced currents in ground-based technological systems, Surveys in geophysics, 23, 71–90, https://doi.org/10.1023/A:1014816009303, 2002.

Pulkkinen, A., Rastätter, L., Kuznetsova, M., Singer, H., Balch, C., Weimer, D., Toth, G., Ridley, A., Gombosi, T., Wiltberger, M., et al.: Community-wide validation of geospace model ground magnetic field perturbation predictions to support model transition to operations, Space Weather, 11, 369–385, https://doi.org/10.1002/swe.20056, 2013.

Rigoti, A., FH, C., NB, T., and AL, P.: Characteristics of the equatorial electrojet determined from an array of magnetometers in N-NE Brazil, Earth, planets and space, 51, 115–128, https://doi.org/10.1186/BF03352216, 1999.

Rout, D., Kumar, A., Singh, R., Patra, S., Karan, D. K., Chakraborty, S., Scipion, D., Chakrabarty, D., and Riccobono, J.: Evidence of Unusually Strong Equatorial Ionization Anomaly at Three Local Time Sectors During the Mother's Day Geomagnetic Storm On 10–11 May 2024, Geophysical Research Letters, 52, e2024GL111 269, https://doi.org/https://doi.org/10.1029/2024GL111269, 2025.

Russell, C.: The dynamics of planetary magnetospheres, Planetary and Space Science, 49, 1005–1030, https://doi.org/10.1016/S0032-0633(01)00017-4, 2001.

Samwel, S. and Miteva, R.: Correlations between space weather parameters during intense geomagnetic storms: Analytical study, Advances in Space Research, 72, 3440–3453, https://doi.org/10.1016/j.asr.2023.07.053, 2023.

Schober, P., Boer, C., and Schwarte, L. A.: Correlation coefficients: appropriate use and interpretation, Anesthesia & analgesia, 126, 1763–1768, https://doi.org/10.1213/ANE.0000000000002864, 2018.

Silva, G., Alves, L., Espinosa, K., Souza, V., da Silva, L., Costa, J., Pádua, M., and Sanchez, S.: Evaluation of dB/dt amplitudes and sources over the Brazilian region during geomagnetic storms in the 2021–2022 biennium, Journal of Atmospheric and Solar-Terrestrial Physics, 258, 106 196, https://doi.org/10.1016/j.jastp.2024.106196, 2024.

Smith, A. W., Rodger, C. J., Mac Manus, D. H., Forsyth, C., Rae, I. J., Freeman, M. P., Clilverd, M. A., Petersen, T., and Dalzell, M.: The Correspondence Between Sudden Commencements and Geomagnetically Induced Currents: Insights From New Zealand, Space Weather, 20, e2021SW002 983, https://doi.org/https://doi.org/10.1029/2021SW002983, 2022.

https://doi.org/10.5194/egusphere-2025-2381
Preprint. Discussion started: 11 June 2025

Soares, G., Yamazaki, Y., Matzka, J., Pinheiro, K., Morschhauser, A., Stolle, C., and Alken, P.: Equatorial counter electrojet longitudinal and seasonal variability in the American sector, Journal of Geophysical Research: Space Physics, 123, 9906–9920, https://doi.org/10.1029/2018JA025968, 2018.

Thomson, A. W., Gaunt, C. T., Cilliers, P., Wild, J., Opperman, B., McKinnell, L.-A., Kotze, P., Ngwira, C. M., and Lotz, S. I.: Present day challenges in understanding the geomagnetic hazard to national power grids, Advances in Space Research, 45, 1182–1190, https://doi.org/10.1016/j.asr.2009.11.023, 2010.

Trivedi, N. B., Vitorello, Í., Kabata, W., Dutra, S. L., Padilha, A. L., Bologna, M. S., de Pádua, M. B., Soares, A. P., Luz, G. S., Pinto, F. d. A., et al.: Geomagnetically induced currents in an electric power transmission system at low latitudes in Brazil: A case study, Space weather, 5, https://doi.org/10.1029/2006SW000282, 2007.

Tulasi Ram, S., Veenadhari, B., Dimri, A., Bulusu, J., Bagiya, M., Gurubaran, S., Parihar, N., Remya, B., Seemala, G., Singh, R., et al.: Super-intense geomagnetic storm on 10–11 May 2024: Possible mechanisms and impacts, Space Weather, 22, e2024SW004 126, https://doi.org/10.1029/2024SW004126, 2024.

Viljanen, A., Nevanlinna, H., Pajunpää, K., and Pulkkinen, A.: Time derivative of the horizontal geomagnetic field as an activity indicator, Annales Geophysicae, 19, 1107–1118, https://doi.org/10.5194/angeo-19-1107-2001, 2001.

Watari, S.: Estimation of geomagnetically induced currents based on the measurement data of a transformer in a Japanese power network and geoelectric field observations, Earth, Planets and Space, 67, 1–12, https://doi.org/10.1186/s40623-015-0253-8, 2015.

Yamazaki, Y. and Maute, A.: Sq and EEJ—a review on the daily variation of the geomagnetic field caused by ionospheric dynamo currents, Space Science Reviews, 206, 299–405, https://doi.org/10.1007/s11214-016-0282-z, 2017.

Zhang, J. J., Wang, C., Sun, T. R., Liu, C. M., and Wang, K. R.: GIC due to storm sudden commencement in low-latitude high-voltage power network in China: Observation and simulation, Space Weather, 13, 643–655, https://doi.org/https://doi.org/10.1002/2015SW001263, 2015.

Zhang, J. J., Yu, Y. Q., Chen, W. Q., Wang, C., Liu, Y. D., Liu, C. M., and Liu, L. G.: Simulation of Geomagnetically Induced Currents in a Low-Latitude 500 kV Power Network During a Solar Superstorm, Space Weather, 20, e2021SW003 005, https://doi.org/https://doi.org/10.1029/2021SW003005, 2022.

Zhou, Y.-L., Lühr, H., and Alken, P.: The sidebands of the equatorial electrojet: General characteristic of the westward currents, as deduced from CHAMP, Journal of Geophysical Research: Space Physics, 123, 1457–1476, https://doi.org/10.1002/2017JA024687, 2018.